



ARCHIVES
of
FOUNDRY ENGINEERING

DOI: 10.1515/afe-2017-0065

Published quarterly as the organ of the Foundry Commission of the Polish Academy of Sciences



ISSN (2299-2944)

Volume 17

Issue 2/2017

137 – 144

Analysis of Crystallization Process of Intensive Cooled AlSi20CuNiCoMg Alloy

R. Władysiak ^{a,*}, A. Kozuń ^b, K. Dębowska ^b, T. Pacyniak ^a^a Department of Materials Engineering and Production Systems, Lodz University of Technology, 1/15 Stefanowskiego Street, 90-924 Lodz, Poland^b Student, Faculty of Mechanical Engineering, Lodz University of Technology, 1/15 Stefanowskiego Street, 90-924 Lodz, Poland

*Corresponding author. E-mail address: ryszard.wladysiak@p.lodz.pl

Received 10.07.2016; accepted in revised form 30.10.2016

Abstract

The work is a continuation of research concerning the influence of intensive cooling of permanent mold in order to increase the casting efficiency of aluminium alloys using the multipoint water mist cooling system. The paper presents results of investigation of crystallization process and microstructure of multicomponent synthetic hypereutectic alloy AlSi20CuNiCoMg. The study was conducted for unmodified silumin on the research station allowing the cooling of the special permanent sampler using a program of computer control. Furthermore, the study used a thermal imaging camera to analyze the solidification process of multicomponent alloy. The study demonstrated that the use of mold cooled with water mist stream allows in wide range to form the microstructure of hypereutectic multicomponent silumin. It leads to higher homogeneity of microstructure and refinement of crystallizing phases of casting.

Keywords: Innovative foundry technologies and materials, Casting die cooling, Water mist, Silumin

1. Introduction

The work is a part of studies on the application of water mist system for multipoint sequential cooling of casting die to produce high strength castings [1,2]. These studies reflect world trends in the research of intensive cooling, rapid crystallization, forming of microstructure and properties of aluminum alloys, magnesium and multi-alloyed alloys. [3-9].

The essence of the research is the efficient cooling by water mist, that intensive cools the mold through evaporation of water droplets on a hot surface of the casting die. An analysis of earlier studies indicate that the cooling of mold enables the shaping of microstructure and achieving high quality casts made of AlSi20 alloy with improved properties.

The verification of silumin's coagulation process preceded by an analysis of knowledge, the phase equilibrium diagrams: Al-Si, Al-

Si-Mg, Al-Co, Al-Si-Co, Al-Ni, Cu-Al-Ni, Al-Si-Ni, Al-Si-Cu Al-Mg₂Si, Al-Cu, Cu-Si, Al-Mg, Mg-Si, Al-Si-Fe, types of reactions and their specific temperatures [10-13]. Cobalt in alloy Al-Co makes the phase Al₉Co₂, that crystallizes in eutectic with α (Al) in the temperature 657° C. Crystallization of Al-Si-Co alloy followed by the transition $L \rightarrow \alpha$ (Al)+ β (Si)+Al₉Co₂. Admixture of ferrum (Al-Si-Co-Fe) causes a change the process into the formula $L \rightarrow \alpha$ (Al)+ β (Si)+Al₉(CoFe)₂. The temperature of these transitions is 575° C [13].

The multicomponent silumins are the subject of research the authors of this publication by many years. Completed earlier work related to the analysis of the crystallization process and microstructure of hypo-, near- and hypereutectic Al-Si alloys with additions Mg, Cu, Ni, Fe, Co, Mo, Cr and W. [14-16]. Identification of the phases, the order of their crystallization and correlation the thermal effects on the ATD curves, phase

transitions and microstructure of silumin developed through selective testing of binary alloys with everyone of additives, and then with the addition of two or more additives simultaneously introduced to the base silumin. These studies indicate that in nonequilibrium conditions the cobalt forms of the phase with copper and iron and nickel $AlCoCu_2FeSi$ and $Al_9(CoNiFeSi)_2$ in α (Al) solution.

The resulting samples were analyzed by linear and surface distribution of elements contained in silumins and with X-ray phase analysis. Examples of test results shown in Figures 1 and 2.

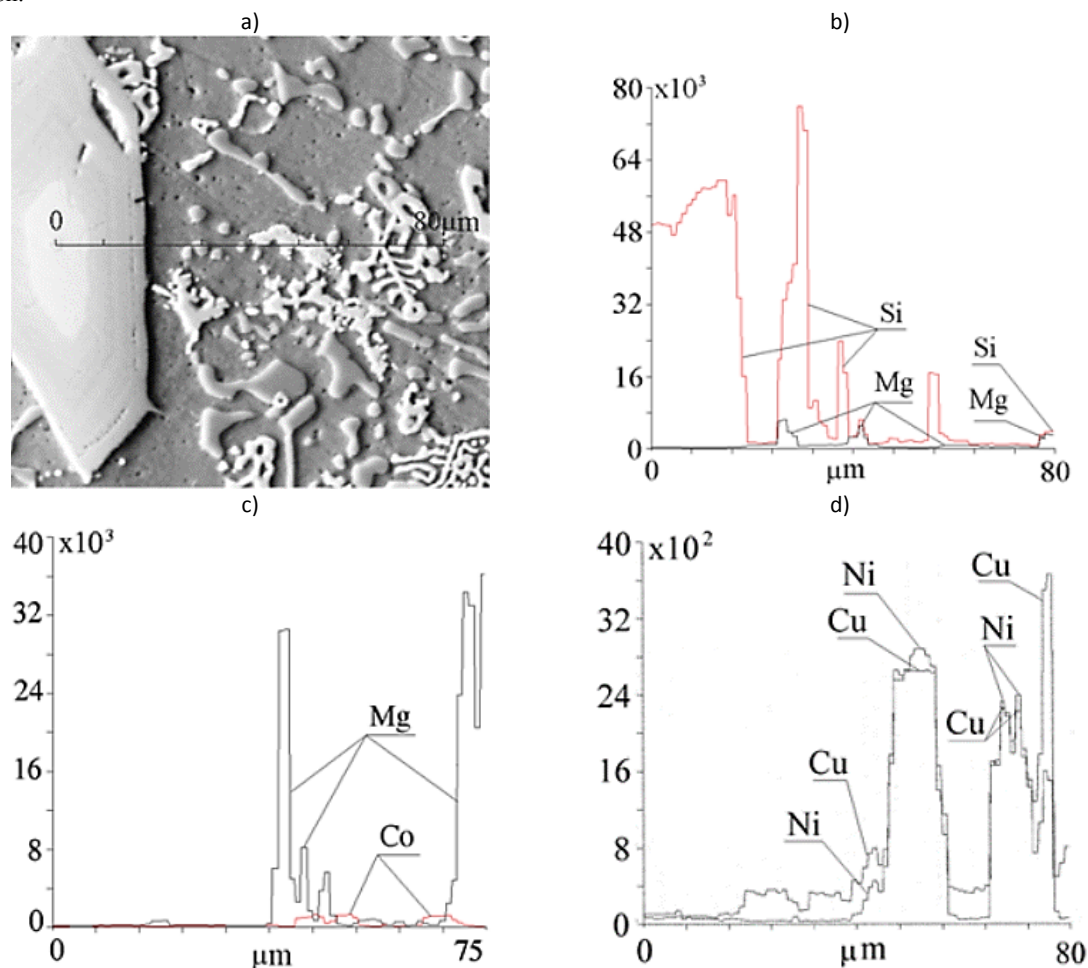


Fig. 1. Microstructure of tested hypereutectic silumin (a) and line-scan profiles of the elements Si (b), Mg(b,c), Co(c), Cu(d), Ni(d)

These results suggest that the presence of Mg, Cu and Ni leads to crystallization of eutectic triple successively with $Al+Mg_2Si+Si$, $Al+Al_3Ni+Si$, $Al+Al_2Cu+Si$ temperature in the range $484 \div 555^{\circ}C$ preceded by preeutectic crystallization of silicon (β) and the next the eutectic ($\alpha+\beta$) with multielement phases. The research also indicates that the content above 0.4% of cobalt causes after the silicon (β) crystals the crystallization of aluminium-based complex multi-phase, such as $Al_9(SiCo)_2$, or the phase $Al(SiFeCoCrMoW)$ observed in structure of multicomponent silumin with additives Co, Cr, Mo, W and for content of $Fe > 0.2\%$. Next are the triple eutectic $\alpha+Al(SiFeCoCrMoW)+\beta$ and even the quadruple eutectic $Al+Al_2Cu+Al(SiMgCuFeCoCrMoW)+Mg_2Si$ [15,16].

The aim of the study was to investigate the effect of water mist cooling on microstructure of hypereutectic synthetic unmodified silumin with elements: copper, nickel, cobalt and magnesium. This type of alloy is used for heavy-duty pistons for combustion engines. They have good casting properties, corrosion resistance, good mechanical properties at elevated temperatures, abrasion resistance, low coefficient of abrasion and thermal expansion [6,3]. The paper presents also the possibility of implementing the infrared thermography for analyzing of silumins solidification process by Thermal and Derivative Analysis (TDA-IR) method [1].

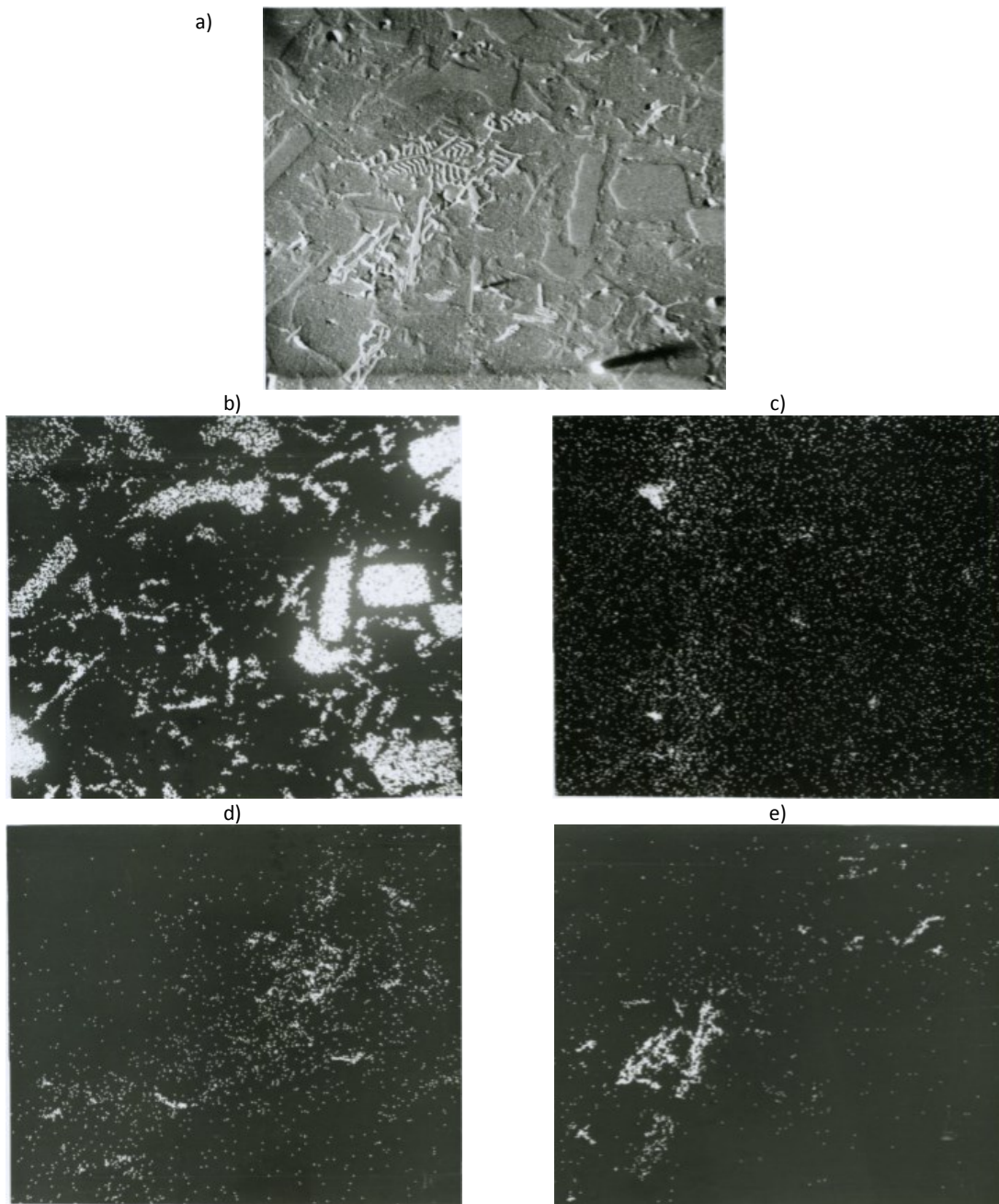


Fig. 2. Microstructure of hypereutectic silumin and surface distribution of its elements: Si (a), Mg (b), Cu (d), Ni (e)

2. Description of the work methodology, materials for research, experiments

The study was conducted on a research stations (shown in Figure 3 and 4) using the ceramic sampler (Fig. 3) and metallic sampler (Fig. 4). They were used in both cases the infrared camera located above the ATD-10 sampler (Fig. 3) and in the thermographic stand (Fig. 4). The metallic sampler was cooled

with water mist delivered by hose of cooling circuit (Fig. 4 point 9) and produced in the device (1,2). At the end, the water mist stream is emitted by cylindrical nozzle towards the external surface of sampler. This sampler was optionally made of aluminium alloy, of cast iron or bronze. Its cone-like shape ensures symmetrical cooling and testing solidification process of Al-alloys with use very small test pieces which weight average is 0,012 kg.

The stream of water mist was controlled using a computerized control system of cooling. The software system includes a set of functions and procedures to monitor and control the course of generating water mist cooling system multichannel using pre-drafted program.

In the sampler were casted the test pieces with use the synthetic silumin AlSi20CuNiCoMg that chemical composition was shown in Table 1. The liquid metal was overheated to the

temperature 800-820°C. The test results of solidification process (Fig. 4) were recorded by infrared camera PI OPRIS 160 and verified by TDA method with use the Crystaldigraph equipment (Fig. 3). Computer software of the infrared camera enables based on the measured signal the development of static thermograms and dynamic thermal cooling curves of objects under the study.

Table 1.

Chemical composition of researched aluminium alloy

Elements, weight %								
Si	Cu	Ni	Co	Mg	Fe	P	Ti	Al
20.21	1.42	1.41	1.25	1.08	0.18	0.01	0.01	rest

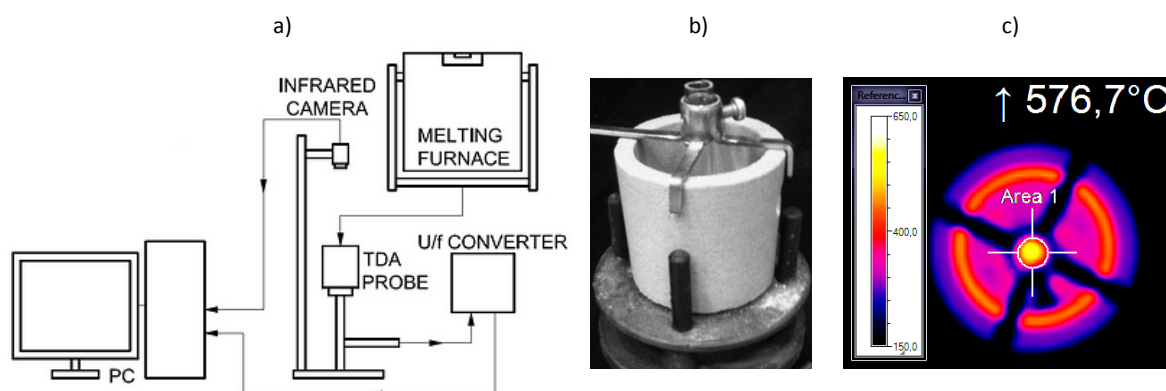


Fig. 3. Scheme of research station (a) and ATD-10 sampler with quartz glass piece: view (b) and thermogram (c) of the sampler during the alloy solidification process

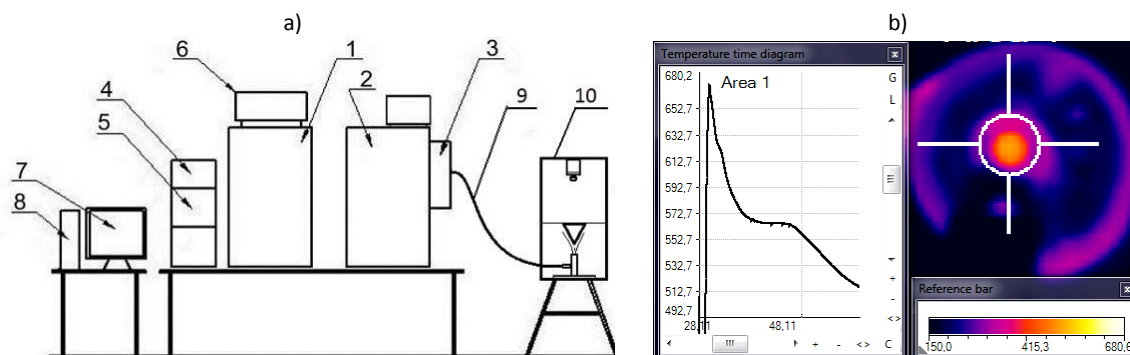


Fig. 4. The scheme of the research station: modules (a): 1, 2 – air and water dosing, 3 – mixing of components, 4, 5 – supplying of air and water solenoid valves, 6 – computer cooling control, 7, 8 – PC, 9 – cooling circuit, 10 – thermographic analysis stand (TDA-IR) and thermographic test results (b) of alloy during the solidification process

These modern cameras work with a high-resolution matrix and with advanced methods of reading and amplification of infrared signal. Features of used camera enable for measurement and recording the temperature in real time with good thermal sensitivity (from 80 mK), high-resolution field (120 x 160 pixel) and with high frequency of measurements (102 Hz). The effect of

water mist cooling on the crystallization and resulting microstructure of silumins was evaluated by using a Nikon microscope MA200.

3. Research results and analysis

In the paper was presented the influence of cooling of casts made of synthetic unmodified silumin AlSi20CuNiCoMg on morphology of crystallizing phases. Tests of crystallization process were made in the ceramic sampler ATD-10 and in metallic sampler made of aluminium alloy.

3.1. Effect of cooling on solidification process

In Figures 3-4 have shown, respectively, representative curves - thermal and derivative of hypereutectic silumin AlSi20CuNiCoMg obtained by TDA method (Fig. 5) and with use the infrared thermography (Fig. 6). Both the tests were conducted for alloy's specimen in sampler ATD-10 which was cooling down naturally in ambient temperature and this process is very closed to equilibrium conditions.

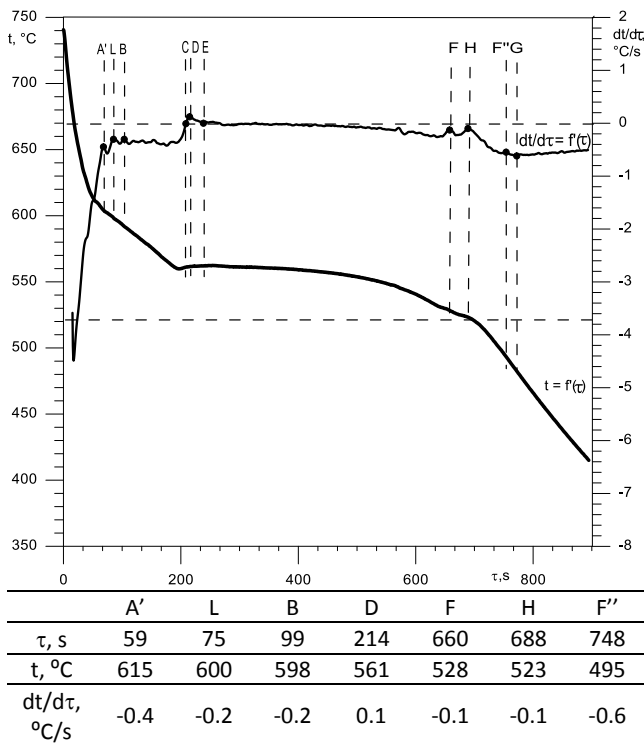


Fig. 5. TDA curves of solidification process of AlSi20CuNiCoMg alloy obtained by TDA method

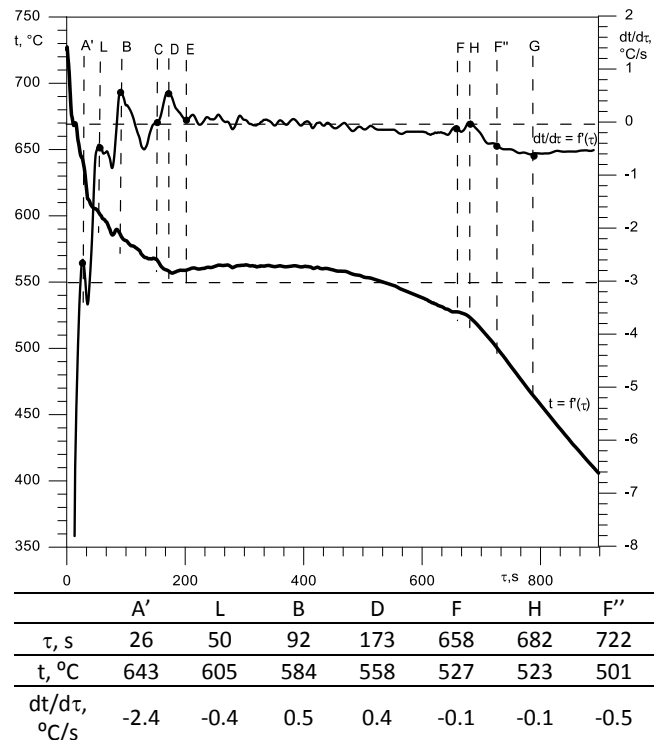


Fig. 6. TDA curves of solidification process of AlSi20CuNiCoMg alloy obtained by thermographic method (TDA-IR)

The crystallization of researched silumins starts from the initial crystallization of silicon crystals that is reflected by thermal effect at the point A', at the temperature $t_{pk} = 615$ °C. This point is a local maximum value in derivative curve $dt/d\tau = -0.4$ °C/s.

The concentration of silicon decreases in the liquid around the large crystals of β (Si) and creates favorable conditions for nucleation of aluminium and cobalt in phases $Al_9(SiCoFe)_2$ and α phase on the existing silicon crystals. Occurrence of the phase $Al_9(SiCoFe)_2$ was suggested by phase equilibrium diagrams, linear distribution of elements and analysis of specimen microstructure. On the crystallization curve, it manifests probably with the thermal effects (peaks) at the point L and B. Farther lowering the temperature causes that the silumin enter into a zone of eutectic coupled growth (from point C) and in terms of irregular eutectic crystallizes eutectic $\alpha(Al)+Al_9(SiCoFe)_2+\beta(Si)$ with maximum thermal effect at the temperature $t_D = 561$ °C. At the end of crystallization of the eutectic there are thermal effects at the point F, H and F''. They reflect crystallization eutectics: $\alpha+Al_3Ni+\beta$, $\alpha+Mg_2Si+\beta$ and $\alpha+Al_2Cu+\beta$, which may contain all elements of alloying additives and iron such as $AlCoCu_2FeSi$ and $Al_9(CoNiMgFeSi)_2$ especially in conditions of intensive cooling of specimen.

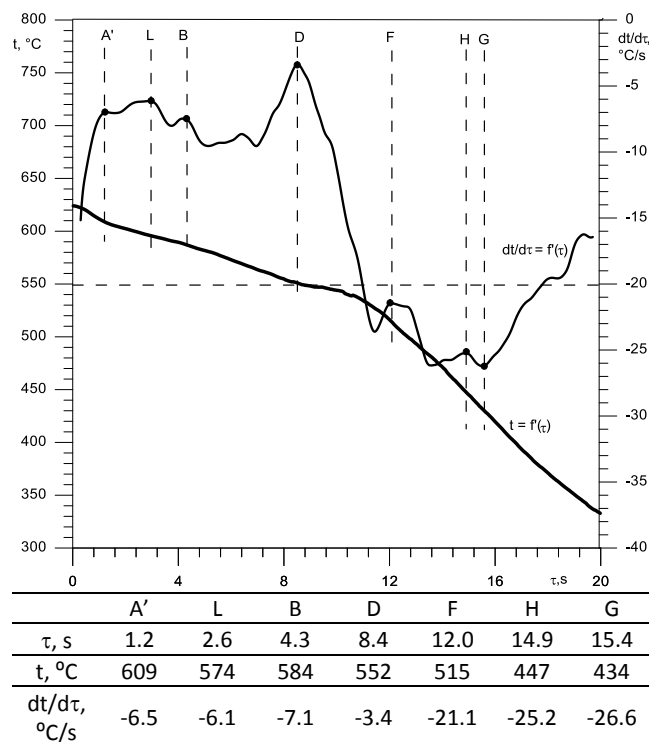


Fig. 7. TDA curves of solidification process of AlSi20CuNiCoMg alloy with water mist cooling obtained by thermographic method (TDA-IR)

In Figure 6 have shown representative thermal and derivative curves of silumin AlSi20CuNiCoMg obtained with use the infrared thermography for alloy's specimen in sampler ATD-10, which was cooling down naturally in ambient temperature. A comparison of the shape and characteristic points the temperature values of thermal curves shows that there are differences between curves made by TDA and TDA-IR method. Moreover, the thermographic method demonstrates clearly bigger initial effects (A', L, B) probably reflecting preeutectical crystallization of phases: β (Si), $Al_9(SiCoFe)_2$ and α (Al). Farther part of crystallization process run according to TDA curves (Fig. 5). Its temperature values demonstrate slight differences in range $0 \div 6$ °C. The end of silumin crystallization is identified in both methods similar cooling rate value $(\frac{dt}{d\tau})_{F,F'} = (-0.1 \div -0.6)$ °C/s.

In Figure 7 have shown representative thermal and derivative curves of silumin AlSi20CuNiCoMg obtained with use the infrared thermography for very small specimen of alloy in metallic sampler with use of cooling the sampler by the water mist stream.

In this case the crystallization of silumin runs many times faster than bigger specimen of silumin in uncooled ceramic sampler (Fig. 3b). The total crystallization time is about 20 seconds at an average cooling rate 12 °C/s in solidification range.

On the curves are clearly visible the thermal effects of crystallization of successive phases β (Si), $Al_9(SiCoFe)_2$ and α (Al) and eutectics: $\alpha(Al)+Al_9(SiCoFe)_2+\beta(Si)$, $\alpha+Al_3Ni+\beta$ and $\alpha+Mg_2Si+\beta$. There is no effect of eutectic $\alpha+Al_2Cu+\beta$. The kinetics of the crystallization is much bigger. Mostly it proceeds with cooling rate about 7 °C/s and in final step process reached $\frac{dt}{d\tau}_G = 27$ °C/s.

3.2. Effect of cooling on microstructure

In Figure 8 have shown a representative microstructure of specimens of silumin AlSi20CuNiCoMg obtained in casting test adequately from ATD-10 sampler cooling naturally at elevated temperature (Fig. 8a), in metallic sampler without cooling (Fig. 8b) and finally in metallic sampler which was cooled by the water mist stream (Fig. 8c).

Microstructure of all silumin specimens contains crystals of silicon (β), significant sized of precipitates $Al_9(SiCoFe)_2$, aluminium dendrites (α) and grains of lamellar eutectic $\alpha+Al_9(SiCoFe)_2+\beta$. Furthermore, the introduction of additives cobalt, nickel, magnesium and copper resulted that in the microstructure occurs phases Mg_2Si , Al_3Ni , Al_2Cu in eutectics $\alpha+Mg_2Si+\beta$, $\alpha+Al_3Ni+\beta$ and $\alpha+Al_2Cu+\beta$.

Changing the type of sampler from a ceramic to a metal one and reducing the sample volume caused increasing the solidification rate and reduces the size of all phases in the alloy structure. Additional these changes of technology caused that there is no triple eutectic $\alpha+Al_2Cu+\beta$ in specimens made in metallic sampler.

In silumin that was cooled the silicon crystals, which crystallized pre-eutectically are many times smaller ($30 \div 70$ μm) especially in comparison to specimen obtained in ceramic sampler ($230 \div 1070$ μm) and have very compacted long-wall shape. Analogical changes are also pre-eutectic separation of phase $Al_9(SiCoFe)_2$. Furthermore, the use of cooling with water mist caused their 2-fold fragmentation and reduction of the share of this phase in the silumin microstructure.

Comparing the specimens shows that the casting from cooled sampler have the refinement of microstructure which is much more for grains of each eutectic of silumin than for pre-eutectic crystals. This is probably due to an increase in crystallization rate due to the increased cooling rate in the melt solidification temperature range.

From a comparison of microstructure obtained in metallic sampler resulted that the cooling with water mist comminuted silicon primary crystals and much more the eutectic grains hypereutectic silumin lamellar. Variety of microstructure morphology is probably the result of changes in the solidification process caused by the intensive cooling of the melt at a rate of ~ 30 °C/s.

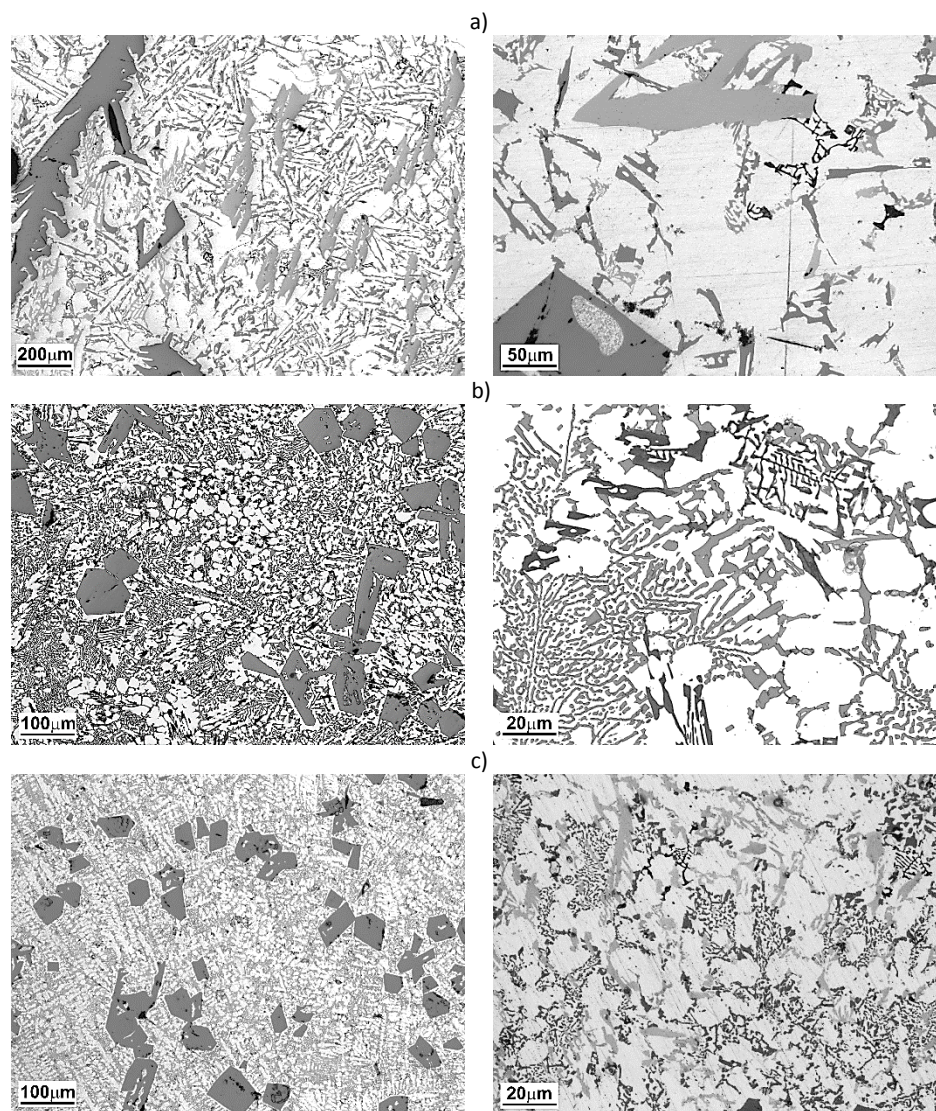


Fig. 8. Microstructure of AlSi20CuNiCoMg alloy poured without cooling in ATD-10 sampler (a) and without cooling in metallic sampler (b) and poured with cooling in metallic sampler (c): β (Si) crystals, α (Al) dendrites (a-c), $\text{Al}_9(\text{SiCoFe})_2$ (a-c) and phases $\text{Al}_9(\text{SiCoFe})_2$, (a-c) Mg_2Si (a-c), Al_3Ni (a-c), Al_2Cu (a, b) that crystallize in eutectics with α (Al) and β (Si).

The research shows that increasing of cooling rate as a result of mold cooling by water mist increases refinement of pre-eutectic long-wall silicon crystals and eutectics of multicomponent piston silumin. These changes are much larger in castings obtained from intensively cooled mold in compare to castings cooled down naturally, in which the primary silicon crystals are larger and do not show the reducing of the lamellas length and edge rounding.

In summary, the studies show that the use the mold cooling with water mist makes possible to shape the several types of microstructures of hypereutectic silumins. A wide range of solidification temperature of hypereutectic silumins increases the potential impact of the change of cooling rate on the size, number and morphology of the crystallizing phases.

4. Conclusions

The study shows that the use of thermographic method and cooling of sampler with water mist:

- provides a quantitative analysis of kinetics the cooling and solidification process,
- enables ATD analysis of crystallization process of hypereutectic AlSi20CuNiCoMg alloy,
- proved that the duration time of entire solidification process of cooled silumin AlSi20CuNiCoMg is about 20 times shorter than uncooled in ceramic sampler,

- enables to achieve the total crystallization time about 20 seconds at an average cooling rate 12 °C/s in solidification range,
- water mist cooling of sampler increases the cooling rate of liquid alloy from $dt/d\tau = -0.6$ °C/s to $dt/d\tau = -26.6$ °C/s and causes significant lowering the temperature of crystallization process of silumin,
- in hypereutectic silumin unmodified reduces size of lamellar eutectic grains and it allows to obtain fine-grained crystals of silicon and $Al_9(SiCoFe)_2$.

References

- [1] Władysiak, R. (2016). Effect of Casting Die Cooling on Solidification Process and Microstructure of Hypereutectic Al-Si Alloy. *Archives of Foundry Engineering*. 16(4), 175-180.
- [2] Władysiak R., Kozuń A., Pacyniak T. (2017). The Effect of Water Mist Cooling on the Solidification, Microstructure and Properties of AlSi20 Alloy. *Archives of Metallurgy and Materials*. 62(1), 187-194.
- [3] Karpe, B., Kosiec, B., Nagode, A. & Bizjak, M. (2013). The Influence of Si and V on the Kinetics of Phase Transformation and Microstructure of Rapidly Solidified Al-Fe-Zr Alloys. *Journal of Mining Metallurgy. Section B: Metallurgy*. 49(1) B, 83-89.
- [4] Roehling J.D., Coughlin D.R., Gibbs J.W., Baldwin J.K., Mertens J.C.E., Campbell G.H., Clarke A.J., McKeown J.T. (2017). Rapid solidification growth mode transitions in Al-Si alloys by dynamic transmission electron microscopy. *Acta Materialia*. 131 (June), 22-30.
- [5] Rapiejko, C., Pisarek, B. & Pacyniak, T. (2017). Effect of intensive cooling of alloy AM60 with chromium and vanadium additions on cast microstructure and mechanical Properties. *Archives of Metallurgy and Materials*. 62(1), 309-314.
- [6] Yamagata, H., Kasprzak, W., Aniolek, M., Kurita, H. & Sokolowski, J.H. (2008). The effect of Average Cooling Rates on the Microstructure of the Al-20% Si High Pressure Die Casting Alloy Used for Monolithic Cylinder Blocks. *Journal of Materials Processing Technology*. 203, 333-341.
- [7] Bamberger, M., Minkoff, I. & Stupel, M.M. (1986). Some Observations on Dendritic Arm Spacing in Al-Si-Mg and Al-Cu Alloy Chill Castings. *Journal of Materials Science*. 21, 2781-2786.
- [8] Qin Bai, Yan-fei Hao, Jiao Wang, Hua Man, Yong-jun Tang, Hui Xu, & Shuang Xia (2012). Effect of Cooling Rate on the Magnetic Properties of Fe53Nd37Al10 Alloy. *International Journal of Minerals Metallurgy and Materials*. 20(5), 440-444.
- [9] Liang C., Chen Z.H., Huang Z.Y., Zu F.Q. (2017). Optimizing microstructures and mechanical properties of hypereutectic Al-18%Si alloy via manipulating its parent liquid state. *Materials Science and Engineering A*. 690 (April) 387-392.
- [10] Pearson, W. B.(1967). Lattice Spacing and Structures of metals and Alloys, *Pergamon Press*.
- [11] Massalski, T.B. (1986). Binary Alloy Phase Diagrams. American Society for Metals. Metals Park, Ohio 44073.
- [12] Mondolfo, L.F. (1976). *Aluminium Alloys; Structure and Properties*. Butterworth, London.
- [13] Czekaj, E. (2011). Piston Nickel-free Silumins with High Dimensional Stability, Foundry Research Institute.
- [14] Pietrowski, S., Szymczak, T., Siemińska-Jankowska B. & Jankowski, A. (2010). Selected Characteristic of Silumins with Additives of Ni, Cu, Cr, Mo, W and V. *Archives of Foundry Engineering*. 10(2), 107-126.
- [15] Pietrowski, S. (1998). Hypereutectic silumin with additives Cr, Mo, W and Co. *Solidification of Metals and Alloys*. 38, 119-118. (Polish).
- [16] Pietrowski, S., Władysiak, R., Pisarek, B. (1999). Crystallization, Structure and Properties of Silumins with Cobalt, Chromium, Molybdenum and Tungsten Admixtures. *Proceedings of the International Conference "Light Alloy and Composites1999"*, 77-83.